Journal of Hydroinformatics

Journal of Hydroinformatics Vol 24 No 6, 1175 doi: 10.2166/hydro.2022.056

Hydrological simulation and prediction of soil erosion using the SWAT model in a mountainous watershed: a case study of Murat River Basin, Turkey

Erkan Karakoyun [a,*] and Nihat Kaya[b]

[a] Faculty of Engineering and Architecture, Muş Alparslan University, Muş 49250, Turkey
[b] Faculty of Engineering, Department of Civil Engineering, Firat University, Elazig 23119, Turkey
*Corresponding author. E-mail: e.karakoyun@alparslan.edu.tr

EK, 0000-0003-2821-9103

ABSTRACT

The Euphrates-Tigris basin in Turkey suffers from sedimentation and erosion problems. The purpose of this study was to estimate streamflow, sediment yield, and identification of soil erosion-prone areas for the Murat River Basin which is the headwater of Euphrates River, with Soil and Water Assessment Tool (SWAT). The model was calibrated and validated with observed streamflow and sediment yield data obtained from two gauging stations. The statistical model performance was evaluated by using NSE, R^2, and PBIAS. NSE values were calculated as 0.57, 0.50 and 0.77, 0.75 for the stations E21A074 and E21A077, respectively, in the monthly streamflow calibration and validation periods. Monthly sediment yield generated the NSE values for stations E21A074 and E21A077 were 0.54, 0.69 and 0.62, 0.35 in the calibration and validation periods, respectively. Spatial analysis indicates that 3.9% of the basin is under very severe (>20 t/ha/y), and 21.3% is under severe (>10 t/ha/y) soil erosion conditions. Most of the soil erosion occurs at the barren land use and in the sub-watersheds with a slope greater than 25%. Overall, the SWAT model satisfactorily simulated the streamflow and sediment yield, and identified the erosion-prone areas at the sub-watershed scale at the Murat River Basin for water resource management.

Key words: Euphrates-Tigris basin, sediment yield, soil erosion, streamflow, SWAT model, watershed management

HIGHLIGHTS

- Streamflow and sediment yield simulated satisfactorily with the SWAT model.
- Soil erosion is much sensitive to land use and slope.
- Barren land with the combination of areas with steep slope generates more soil erosion.
- This study can help watershed managers to prioritize measures.

GRAPHICAL ABSTRACT

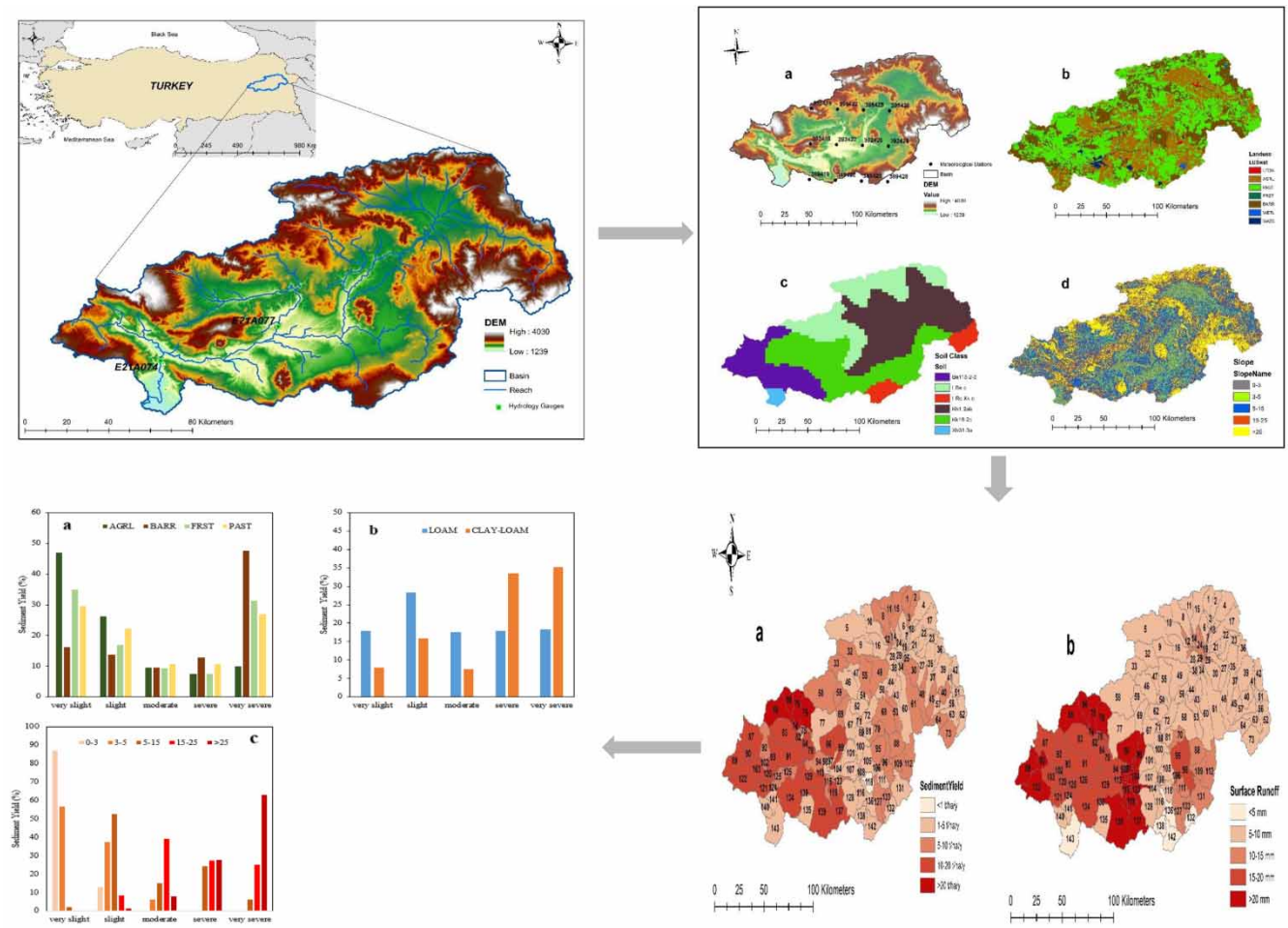

1. INTRODUCTION

Sedimentation is the main problem for dams and hydraulic structures which results in the reduction of the dam's usable storage volume in the determination of capacity and operation (Morris & Fan 1998). The sedimentation occurring in the reservoir affects the water quality both chemically and physically (Alemayehu *et al.* 2014). Chemically, sediments act as a distribution mechanism for particular pollutants degrading the water quality within a reservoir. Physically, sedimentation reduces the useful life of the reservoir (Juracek & Stiles 2010). According to Mahmood (1987), each year reservoirs around the world lose their storage volume by 0.5–1%. In Turkey, a lack of measurements for erosion control and land use results in the accumulation of sediments and reduces the capacity of the dam's economic life such as in Medik Dam, Akkaya Dam, and Cubuk-1 Dam (Koycegiz *et al.* 2021). Each year 154 million tons of sediment are transported by the rivers of Turkey and 84 million tons of this is carried only by the rivers in the Euphrates-Tigris basin (CEM 2018).

In most instances, the cause of sedimentation in reservoirs is soil erosion and occurs mainly on erodible soils, high terrain slopes, and due to intensive rainfall (Beskow *et al.* 2009). Soil erosion caused by water removes fertile soil layer from the surface, causing accumulation in rivers, lakes, and reservoirs, and can be caused to agricultural, environmental, and economic problems (Wu & Chen 2012; Chandra & Rabin 2019). Moreover, because of climate change, land use change, and human interference, soil erosion has become challenging issue (Zare *et al.* 2017; Chakrabortty & Chandra 2020; Pal *et al.* 2021). According to Panagos *et al.* (2021), mean soil loss rates caused by water erosion would rise by 13–22.5% in agricultural areas of European Union countries compared with 2016 baseline by 2050. However, given a specific location in the watershed, erosion depends on many factors such as regional precipitation patterns, soil texture, land use and management, and

topography (Panagos *et al.* 2015; Roy *et al.* 2020). Consequently, case studies are encouraged to develop watershed management and soil and conservation studies (Sohoulande Djebou 2018), so efforts can be focused to preserve soil and water resources at the sub-basin scale to minimize the negative impact of soil erosion on the environment.

In order to estimate accurate and reliable streamflow, sediment carried from the land surface into the rivers, and identify the erosion-prone areas to suggest the best management practices in the watershed, hydrological models are used (Briak *et al.* 2016; Chakrabortty *et al.* 2022). These models are used effectively to estimate water quality, sediment yield, streamflow, the effects of climate, and land-use changes (Abouabdillah *et al.* 2014; Abbaspour *et al.* 2015; Ricci *et al.* 2018; Van Liew & Mittelstet 2018). The Soil and Water Assessment Tool (SWAT) developed by Arnold *et al.* (1998) is a physically based hydrological model that is used widely in literature for different purposes. Several researchers have been studied with SWAT for simulating runoff (Jakada & Chen 2020), sediment yield (Rodríguez-Blanco *et al.* 2016), water quality (Abbaspour *et al.* 2007; Qi *et al.* 2020), determine soil erosion areas (Vigiak *et al.* 2015; Dutta & Sen 2018; Abdelwahab *et al.* 2018; Daramola *et al.* 2019), and in different watersheds across the globe. Additionally, the model has been applied to assess the impact of climate change (Zhang *et al.* 2014; Tzoraki *et al.* 2015; Pal & Chakrabortty 2019; De Girolamo *et al.* 2022); land use, and land cover change effect assessment (Jodar-Abellan *et al.* 2019).

Soil is among the most important natural resources (Chakrabortty *et al.* 2020). Besides, land degradation due to soil loss has a negative impact on crop production and agriculture in many countries around the world (Pal & Shit 2017). According to a global study (Wuepper *et al.* 2020), Turkey is among the countries that are more severely affected by soil erosion. Turkey is a mountainous country with the mean elevation is nearly 1,250 m and 62.5% of total surface has more than 15% slope (Imamoglu & Dengiz 2017). Hilly topography and vegetation are among the two most important factors of soil erosion causing land degradation and nearly 12.7% of the total area of Turkey is exposed to severe and very severe soil erosion (CEM 2018). In the Euphrates-Tigris basin, which has Turkey's largest and highest water potential basin, occurs nearly a quarter of the total erosion of Turkey and half of the total sediment yield of its (CEM 2018). In this case, sustainable management and a convenient eco-friendly solution should take account for the Euphrates-Tigris basin for reducing the sedimentation in the reservoir and identifying the erosion-prone areas.

Several studies have been conducted by using the SWAT model around the world, but these studies are limited in Turkey (Guzel 2010; Akiner & Akkoyunlu 2012; Cuceloglu *et al.* 2017; Yıldırımer 2018; Peker & Sorman 2021) especially in the Euphrates-Tigris basin. The Murat River Basin is one of the headwater of Euphrates River and it is the source of several large dams in downstream. Agriculture and livestock are the main livelihoods of the region. Hence, the streamflow, sediment yield, and soil erosion model analysis can be a suitable tool in this basin for watershed management planners. To the best of our knowledge, there is no study in the Murat River Basin with spatial and temporal analysis of sediment yield and soil erosion performed. Hence, the novel contribution of this study will guide the hydrologist, water resource planners, and watershed management applications in the Murat River Basin. For these reasons, the SWAT model has been selected as a tool to simulate hydrological processes and sediment yield. Besides, the detailed objectives of this study are given as follows: (1) assessing the applicability of the SWAT model for the hydrological analysis in the Murat River Basin, (2) compare the model prediction of streamflow based on daily time interval, and (3) determine soil erosion-prone areas within the studied watershed where measures to reduce soil erosion are needed.

2. MATERIALS AND METHODS

2.1. Study area

The study area, called as Murat River Basin, is located on the upper part of the Euphrates-Tigris basin (Figure 1). The length of the Murat River is 720 km and merges with the Karasu River then generate the Euphrates River which is the longest river in Western Asia. The river has an important social-economic role in the region since there are highly important dams (Keban Dam, Ataturk Dam, etc.). Discharge and sediment load data from two gauging stations (E21A074, 39°02′N; 41°31′E; 17,435 km^2 drainage area, and E21A077, 39°13′N; 42°10′E; 2,995 km^2 drainage area) were used to calibrate the SWAT model, which are located on the Murat River Basin (Figure 1). The area of the Murat River Basin is 17,865 km^2. The elevation is between 1,239 and 4,033 m above the mean sea level with the mean elevation being 1,945 m. The watershed is mountainous and has varying topography with steep slopes and the average slope is 12.6%. High altitude and the differences in the elevation range in combination with steep slope would have an effect on sediment yield and soil erosion loss. The dominant

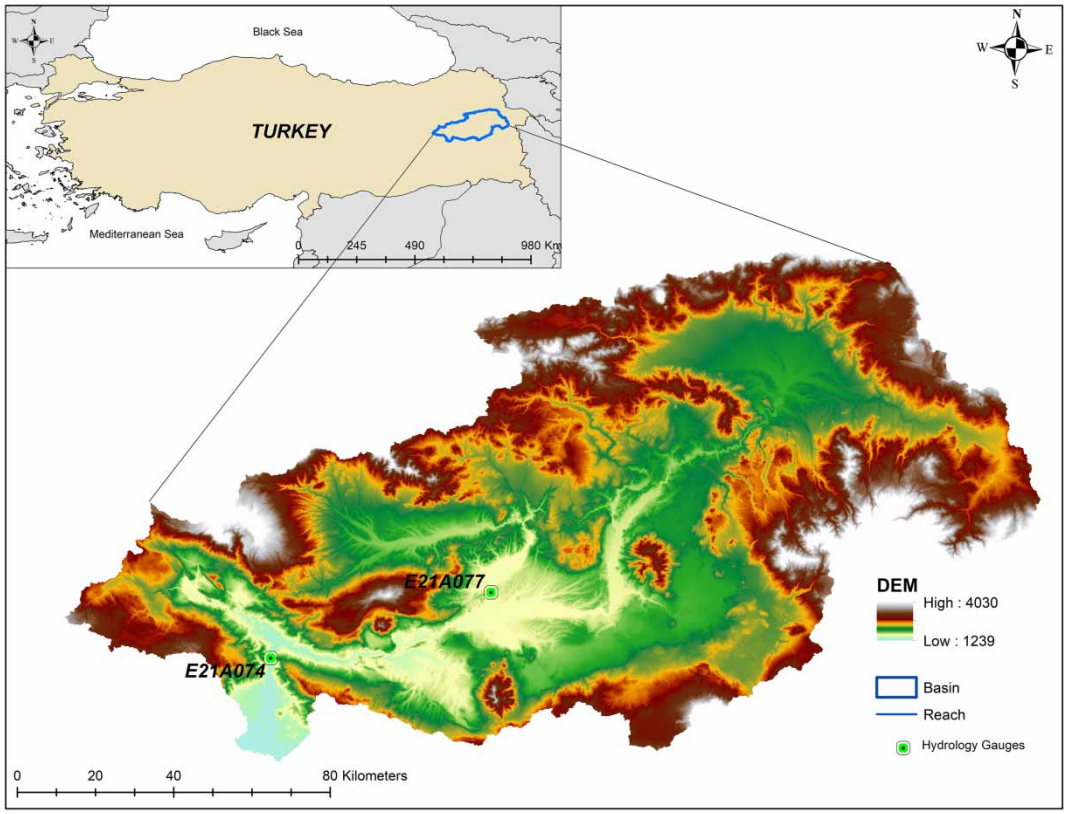

Figure 1 | Location map of the Murat River Basin.

land use classification is pasture followed by agricultural production (CORINE 2012) and, as for the soil texture, different types of Kastanozems are the major soil groups in the study area (FAO/UNESCO).

The spring months, March to May, is the rainy season of the watershed and occurred the peak flows in this period. The winter is generally snowy where snowmelt is the main source feeding the river and the maximum snowmelt also occurred in the spring months. The yearly average precipitation of the studied watershed is 774.5 mm. The maximum temperature was recorded in the studied period (2005–2013), in August 2006 as 38.1 °C and the minimum temperature in January 2012 as −33.7 °C.

2.2. SWAT model description

ArcSWAT is a user-friendly software program which is an extension of ArcGIS-ArcView with a graphical user input interface for SWAT.

The SWAT is developed by the United States Department of Agriculture (USDA)-Agricultural Research Service (ARS) as a hydrological model to estimate the impact of land management practices on the sediment yield, water, nutrients, and water quality in the large basins (Arnold *et al.* 1998). The SWAT is a computationally effective physically based continuous time model that can perform on a daily to yearly time interval. The Digital Elevation Model (DEM) is used in the SWAT model to delineate the basin boundary and to divide the basin into sub-basins (Arnold *et al.* 2012). Further, each sub-basin is subdivided into the hydrological response units (HRUs) which consist of the unique combination of soil, land use, and slope properties (Arnold *et al.* 2012). The hydrological cycle in the SWAT model is based on the water balance Equation (1) (Neitsch *et al.* 2005).

$$\mathrm{SW}_t = \mathrm{SW}_0 + \sum_{n=1}^{t} (R_{\mathrm{day}} - Q_{\mathrm{surf}} - E_a - W_{\mathrm{seep}} - Q_{\mathrm{gw}}) \quad (1)$$

where SW_t is the soil water content (mm), SW_0 is the initial soil water content (mm), R_{day} is the precipitation (mm), Q_{surf} is the surface runoff (mm), E_a is the evapotranspiration (mm), W_{seep} is the amount of water entering the vadose zone from the soil profile (mm), Q_{gw} is the return flow (mm), and t is the time.

The SWAT model has been widely used to predict the sediment yield in previous studies (Gull *et al.* 2017; Tesema & Leta 2020; Borrelli *et al.* 2021). Runoff would be the critical factor with transporting capacity for controlling sediment yield (Mutchler *et al.* 1998). Modified Universal Soil Loss Equation (MUSLE) is used to predict the sediment yield and soil erosion for each sub-basin (Williams 1975) as given by Equation (2).

$$\text{Sed} = 11.8*(Q_{surf}*q_{peak}*\text{area}_{hru})^{0.56}K_{USLE}*C_{USLE}*P_{USLE}*LS_{USLE}*\text{CFRG} \quad (2)$$

where Sed is the sediment yield on a given day (tons), Q_{surf} is the surface runoff volume (mm/ha), q_{peak} is the peak runoff rate (m^3/s), area_{hru} is the area of HRU (ha), K_{USLE} is the USLE soil erodibility factor, C_{USLE} is the USLE soil cover factor, P_{USLE} is the USLE support practice factor, LS_{USLE} is the topographic factor, slope length, and slope steepness as dimensionless factor, and CFRG is the coarse fragment factor.

The peak runoff rate is defined by the SWAT model as follows:

$$Q_{peak} = \frac{A*Q_{surf}*\text{Area}}{360*t_{conc}} \quad (3)$$

where Q_{peak} is the peak runoff rate (m^3/s), A is the fraction of total rainfall that occurs during the time of concentration, Area is the HRU area (ha), and t_{conc} is the time of concentration (h).

2.3. SWAT model inputs

SWAT is a physically based model that requires a great deal of input data such as topographic, soil properties, land use/cover, management practices, hydrological, and meteorological data (Table 1). In this study, SWAT 2012 with an ArcGIS 10.7 (Esri 2019) interface was used to perform the simulation. The model uses the DEM to determine the direction of the water flow and the watershed boundaries. The DEM was obtained from ASTER Global Digital Elevation Model V3 with a 30 m spatial resolution (NASA 2019). Before adding the DEM into the ArcSWAT, the edited DEM was projected to WGS84 UTM Zone-38N as a study area location. Then, the watershed was delineated to analyze the drainage pattern of the land surface and then subdivided into 143 sub-watersheds. The elevation range found for the watershed varies from 1,239 to 4,030 m as seen in Figure 2(a).

The land use/cover map was obtained from the Coordination of Information on the Environment Land Cover datasets (CORINE 2012) with a 100 m resolution. Since the study period was between 2005 and 2013, the year of land cover data was chosen as 2012 to better represent the calibration/validation period. The dominant land cover was observed as a pasture with a portion of 47.43% and agricultural land (26.48%), barren (22.91%), water (1.41%), forest (0.33%), residential (1.02%), and wetland (0.42%) as seen in Figure 2(b). The soil map was obtained from the Harmonized World Soil Database v1.2

Table 1 | SWAT model input table

Data type	Description	Information	Data source
Topography	Digital Elevation Map	30 m-resolution	USGS–ASTER GDEM
Land Use/Cover Map	Land Use/Cover	100 m-resolution	Coordination of Information on the Environment Land Cover dataset (CORINE 2012)
Soil Map	Soil Type	6 soil profiles	FAO-UNESCO
Hydrologic	Observed Streamflow and Sediment Data	2 stations (E21A074, E21A077)	Turkish State Hydraulic Works (DSI)
Meteorologic	Precipitation, Temperature, Relative Humidity, Wind Speed, and Solar Radiation	12 stations	The National Centers for Environment Prediction (NCEP) Climate Forecast System Reanalysis (CFRS)

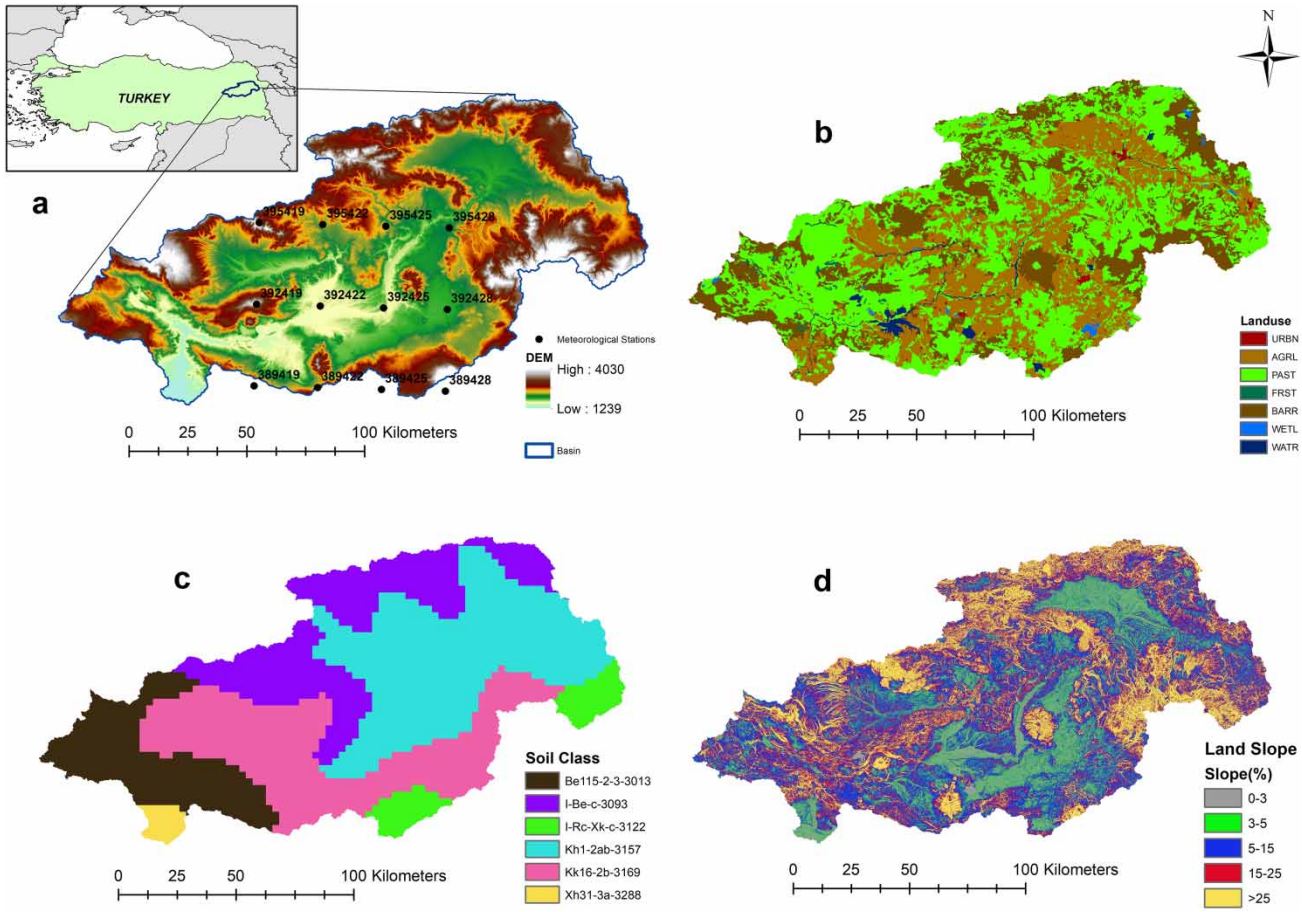

Figure 2 | (a) Topographic map and location of climate station on the watershed, (b) land use/cover area classification, (c) soil types classification, and (d) slope classification of the Murat River Basin.

(HWSD) developed by the Food and Agriculture Organization (FAO/UNESCO). The grid-based soil data obtained from the Digital Soil Map of World (DSMW) database was added into the model in the same projection as the DEM and land use/land cover data after adding the properties of the DSMW soils to the model database file. According to the FAO's soil classification system, Eutric Cambisols (Be115-2-3), Lithosols-Eutric Cambisols (I-Be-c), Lithosols-Calcaric Regosols-Calcic Xerosols (I-Rc-Xk-c), Haplic Kastanozems (Kh1-2ab), Calcic Kastanozems (Kk16-2b), and Haplic Xerosols (Xh31-3a) were defined in the study area (Figure 2(c)). The whole watershed was categorized into five slope classes using the ArcSWAT interface (Figure 2(d)). Then, all the maps, land use/cover, soil, and slope were overlaid to create the HRU's. Since the studied watershed is snow-dominated mountainous, ten elevation bands were added to increase the model accuracy. The purpose of this process is to enable the model to simulate snowfall and snowmelt separately for each elevation band by taking into account the changes in precipitation and temperature depending on the altitude in each sub-basin (Abbaspour *et al.* 2007). Previous studies also refer that adding elevation bands increases the model's accuracy for mountainous watersheds and there is no certain number of elevation bands recommended (Peker & Sorman 2021).

Due to the lack of available datasets (such as relative humidity, wind speed, and solar radiation) for the study area, globally available weather data were used for SWAT modeling. Climate Forecast System Reanalysis (CFSR) by the National Centers for Environmental Prediction was used for climate data. Twelve points were detected for obtaining climate data from CFSR in the studied area (Figure 2(a)). The observation data, suspended sediment, and discharge were obtained from Turkish State Hydraulics Works (DSI). But, the agency collects the suspended sediment sampling once or twice a month from the gages. Therefore, these data may not be sufficient for annual sediment estimates. The LOADEST estimator, version 2012 (Runkel *et al.* 2004) was used to convert suspended sediment data to monthly sediment load. LOADEST can be used to

generate a regression model for predicting constituent loads in streams and rivers. The model estimates constituent loads using three statistical methods. In this study, the Adjusted Maximum Likelihood Estimation (AMLE) method was used. The sediment load outputs obtained from the LOADEST estimator used as an input for the SWAT model. After entering all input parameters into the interference, the SWAT model was set and run on a daily and monthly time period for the years between 2005 and 2013 which is one year selected as a warm-up period.

2.4. Sensitivity analysis, model calibration and validation

Several parameters can be used for calibration and validation procedures. However, some parameters are affecting the targeted variable more than the other parameters, defined as sensitive parameters (Panda *et al.* 2021). SWAT Calibration Uncertainty Procedure (SWAT-CUP) program was used to compare flow and sediment prediction in this study. SWAT-CUP program is capable of performing sensitivity analysis, calibration, validation, and uncertainty analysis of the SWAT model (Abbaspour 2015). Besides, to predict the parameters about streamflow and sediment yield, the Sequential Uncertainty Fitting Version 2 (SUFI-2) algorithm was selected (Abbaspour *et al.* 2004). Two statistical parameters as p-factor and r-factor were used in the SUFI-2 algorithm. p-factor (range 0–1) is the percentage of the actual data covered 95 PPU (95% prediction uncertainty). In other words, (1 – p-factor) can be defined as a model error (Abbaspour *et al.* 2017). The r-factor (range 0–∞) is the ratio of the average thickness of 95 PPU to the standard deviation of observed data. The results having higher p-factor and lower r-factor represent better model performance (Abbaspour *et al.* 2007). The reference p-factor and r-factor ranges to be used for sediment and streamflow according to the study of Abbaspour (2022) are given in Table 2.

In sensitivity analysis, *p*-value and *t*-stat statistical parameters are used to assess sensitive parameters in the SUFI-2 algorithm. While the *p*-value approaching zero and larger absolute *t*-stat values are considered more sensitive the parameters that entered to SWAT-CUP. In this study, the Latin Hypercube One Factor-At-a Time (LH-OAT) (van Griensven & Meixner 2006) sampling technique was used to perform global sensitivity analysis. The SWAT-CUP model was performed with 500 simulations with 25 parameters. Fifteen most sensitive parameters were selected for streamflow calibration and validation process and three hydrological parameters selected for after streamflow calibration for sediment calibration and validation (Table 3).

Calibration can be defined as adjusting model parameters to achieve the best simulation match with observation data. In this study, the parameters which are precipitation lapse rate (PLAPS) and temperature lapse rate (TLAPS) were fixed and removed from the calibration procedure before starting the calibration procedure with the sensitive parameters. Then, the same process was applied for the following snow parameters: snowfall temperature (SFTMP), snowmelt base temperature (SMTMP), maximum and minimum melt rate for snow during the year (SMFMX, SMFMN), and snowpack temperature lag factor (TIMP). Finally, the calibration and validation procedure was performed with 500 simulations with selected sensitive parameters.

All kinds of soil protection methods, such as terracing, grazing, and transverse structure, are considered as inputs to support practice factor (USLE_P). USLE_P value was assigned to be 1, since there was no protection method in the studied area. The value of soil erodibility factor, USLE_K, was set the value of 0.347 after the calibration. Channel cover factor (CH_COV) has an impact on the soil loss from channels (Dutta & Sen 2018) and it was set to 0.005.

In this study, the calibration and validation of the SWAT model were applied with the observed data obtained from two gauging stations (E21A074 and E21A077) on the Murat River basin. The calibration and validation period were determined between 2006–2010 and 2011–2013, respectively, while 2005 was selected as the warm-up period.

The monthly average discharge and sediment data were used based on monthly time interval in the model for selected two gauging stations. Besides, only daily discharge data was used for the daily-based model. 500 simulations were performed with Nash–Sutcliffe Efficiency (NSE) that was selected as an objective function until reach the satisfactory criteria. The model evaluation methods given by Moriasi *et al.* (2007), who defined standards for model evaluation and presented value

Table 2 | The range of uncertainty analysis for streamflow and sediment simulation (Abbaspour 2022)

Uncertainties	Streamflow	Sediment
p-factor	≥0.7	≥0.4
r-factor	≤1.5	≤2

Table 3 | SWAT-CUP parameters for streamflow calibration and their fitted values

Rank	Sensitive parameters	Initial range	Fitted value
	Streamflow		
1	r_CN2 (SCS curve number)	−0.3 to 0.01	−0.11
2	v_ESCO (Soil evaporation compensation factor)	0.25–0.8	0.29
3	v_ALPHA_BF (Baseflow alpha factor)	0–0.4	0.32
4	v_CANMX (Maximum canopy storage)	10–100	71
5	v_CH_K2 (Effective hydraulic conductivity in main channel alluvium)	50–100	101.71
6	v_OV_N (Manning's "n" value for overland flow)	0–0.75	0.24
7	v_CH_N2 (Manning's "n" value for the main channel)	−0.01 to 0.3	−0.004
8	v_RCHRG_DP (Deep aquifer percolation fraction)	0–1	0.27
9	r_SOL_Z (Depth from soil surface to bottom of layer)	−0.2 to 0.2	−0.05
10	v_GW_DELAY (Groundwater delay)	100–300	269
11	v_EPCO (Plant uptake compensation factor)	0–0.6	0.04
12	r_SOL_AWC (Available water capacity of the soil layer)	−0.2 to −0.01	−0.15
13	v_FFCB (Initial soil water storage expressed as a fraction of field capacity water content)	0.15–0.55	0.18
14	v_SURLAG (Surface runoff lag time)	1–24	17.65
15	v_SLSOIL (Slope length for lateral subsurface flow)	0–150	128.75
	Sediment		
1	r_USLE_K (USLE equation soil erodibility (K) factor)	0–0.2	0.144
2	v_CH_COV1 (Channel erodibility factor)	0–0.1	0.005
3	r_ADJ_PKR (Peak rate adjustment factor for sediment routing in the sub-basin)	0–0.2	0.018

v: existing parameter value is to be replaced by a given value.
r: existing parameter value is multiplied by (1 + given value).

ranges and corresponding performance ratings for suggested statistical parameters, are referred to in this study (Moriasi *et al.* 2007; Table 4). According to their study, the NSE and R^2 (coefficient of determination) value greater than 0.5 are the acceptable values for streamflow and sediment models.

After reaching the valid statistical criteria of streamflow estimation, sediment yield can be calibrated and validated because the runoff and streamflow is the main driven factor of sediment transportation (Arnold *et al.* 2012). After having a satisfactory calibration results, the validation processes were performed with the same calibrated parameters to simulate streamflow and sediment yield. The average and standard deviation of the streamflow and sediment yield data used in the calibration and validation period should not be much different from each other (Abbaspour *et al.* 2017). The statistical correlation obtained between calibration and validation data for two gaging stations that are used in this model given in Table 5.

Results from calibration and validation must meet some criteria to be acceptable (Table 4). Three statistical evaluation criteria including R^2, NSE (Nash & Sutcliffe 1970), and Percent Bias (PBIAS) (Gupta *et al.* 1999) were selected to evaluate the performance of the SWAT model based on the accuracy of predicted and observed streamflow and sediment yield.

Table 4 | The performance criteria of recommended statistics for streamflow and sediment (Moriasi *et al.* 2007; Ayele *et al.* 2017)

			PBIAS (%)	
Performance rating	R^2	NSE	Streamflow	Sediment
Very good	$0.7 < R^2 < 1$	$0.75 < NSE < 1.00$	$PBIAS < \pm 10$	$PBIAS < \pm 15$
Good	$0.6 < R^2 < 0.7$	$0.65 < NSE < 0.75$	$\pm 10 < PBIAS < \pm 15$	$\pm 15 < PBIAS < \pm 30$
Satisfactory	$0.5 < R^2 < 0.6$	$0.50 < NSE < 0.65$	$\pm 15 < PBIAS < \pm 25$	$\pm 30 < PBIAS < \pm 55$
Unsatisfactory	$R^2 < 0.5$	$NSE < 0.50$	$PBIAS > \pm 25$	$PBIAS > \pm 55$

Table 5 | Mean sediment loads and mean streamflow recorded at the two gauging stations for the calibration and validation periods

		Sediment Load (tons)		Streamflow (m^3/s)	
		Mean	Standard Deviation	Mean	Standard Deviation
E21A077	Calibration (2006–2010)	1,855	4,145	24.7	29.1
	Validation (2011–2013)	1,451	3,428	22.9	25.4
E21A074	Calibration (2006–2009)	3,960	5,185	108	155
	Validation (2010–2011)	5,595	5,064	149	142

3. RESULTS AND DISCUSSION

3.1. Streamflow outputs

The created SWAT model was calibrated and validated for streamflow and sediment yield on monthly and daily basis. Figure 3 indicates the hydrograph of observed and simulated streamflow that was obtained from calibration and validation for the monthly and daily time intervals for the two gaging stations. The performance criteria including NSE values were found as 0.77 and 0.75, R^2: 0.77 and 0.78, and PBIAS: −6.6 and −3.1% in the calibration and validation period, respectively, at the station E21A077 for monthly time scale. The model uncertainties, p-factor was found as 0.72 and 0.86 while the r-factor was 1.14 and 1.22. According to Abbaspour (2022), the obtained results of p-factor and r-factor are satisfactory (Table 2).

Besides, for the station E21A074, the NSE was found 0.57 and 0.50, R^2 was 0.57 and 0.53, and PBIAS was −7.4 and 15.6% (Table 6). According to the evaluation criteria by Moriasi *et al.* (2007), the performance of the model is in the acceptable range for the studied watershed (Table 4). The same procedures were applied to the daily-based simulation. The model produced less effective performance values on the daily simulation than on the monthly simulation. Similar results were found in the literature as well (Yang *et al.* 2016; Duru *et al.* 2018). However, the results are still in the acceptable ranges with NSE: 0.56, 0.55, R^2: 0.57, 0.56, and PBIAS: −15, 1.2% in calibration and validation periods, respectively, for the station E21A074 (Table 6). The detailed results of calibrated and validated streamflow for two stations are given in Table 6.

The scatterplot was created between observed versus simulated streamflow to define the correlation (Figure 4). 56 and 77% correlation values were calculated between observed and simulated streamflow for monthly based simulation while 57 and 47% correlation for daily-based simulation at the stations E21A074 and E21A077, respectively (Table 6).

3.2. Sediment yield outputs

After calibrating and validating streamflow, calibration and validation were computed for the sediment yield estimation based on monthly time intervals at the selected two stations. For simulated monthly sediment yield the following statistic parameters were found at the station E21A074: NSE as 0.54, 0.69, R^2: 0.67, 0.68, PBIAS: −33.8, 4.6%, p-factor: 0.83, 0.42, and r-factor: 2.38, 0.43 for the calibration and validation periods, respectively (Table 7). Results show that sediment simulation was well performed at station E21A074. For the station E21A077, the values of NSE: 0.62, 0.35, R^2: 0.68, 0.56, PBIAS: −3.2, −77.2%, p-factor: 0.77, 0.20, and r-factor: 0.79, 0.49 were found at the calibration and validation periods, respectively. Although the statistical results were produced sufficiently in the calibration period, it was below the acceptable ranges in the validation period (Figure 5). This could results from observational data error, modeling error or human interaction such as mining and quarry on the watershed (Daramola *et al.* 2019). There are many quarries and concreate stations observed in the upper part of the watershed. These findings can explain the easier transport of sediment particles with runoff into the stream that is not captured by the model.

The scatterplot of observed and simulated sediment load data is shown in Figure 6. The correlation was found 56 and 68% between observed and simulated sediment load data at stations E21A074 and E21A077, respectively.

3.3. Examination of the SWAT model results

The results obtained from the SWAT model were accepted as satisfactory for simulating streamflow and sediment yield. This study also investigates the soil erosion-prone areas at the sub-basin scale that is important for water management practices with the SWAT model. Some management practices could be applied in the basin to reduce the impact of soil erosion. The soil erosion was divided into five classes: very slight (<1 t/ha/y), slight (1–5 t/ha/y), moderate (5–10 t/ha/y), severe

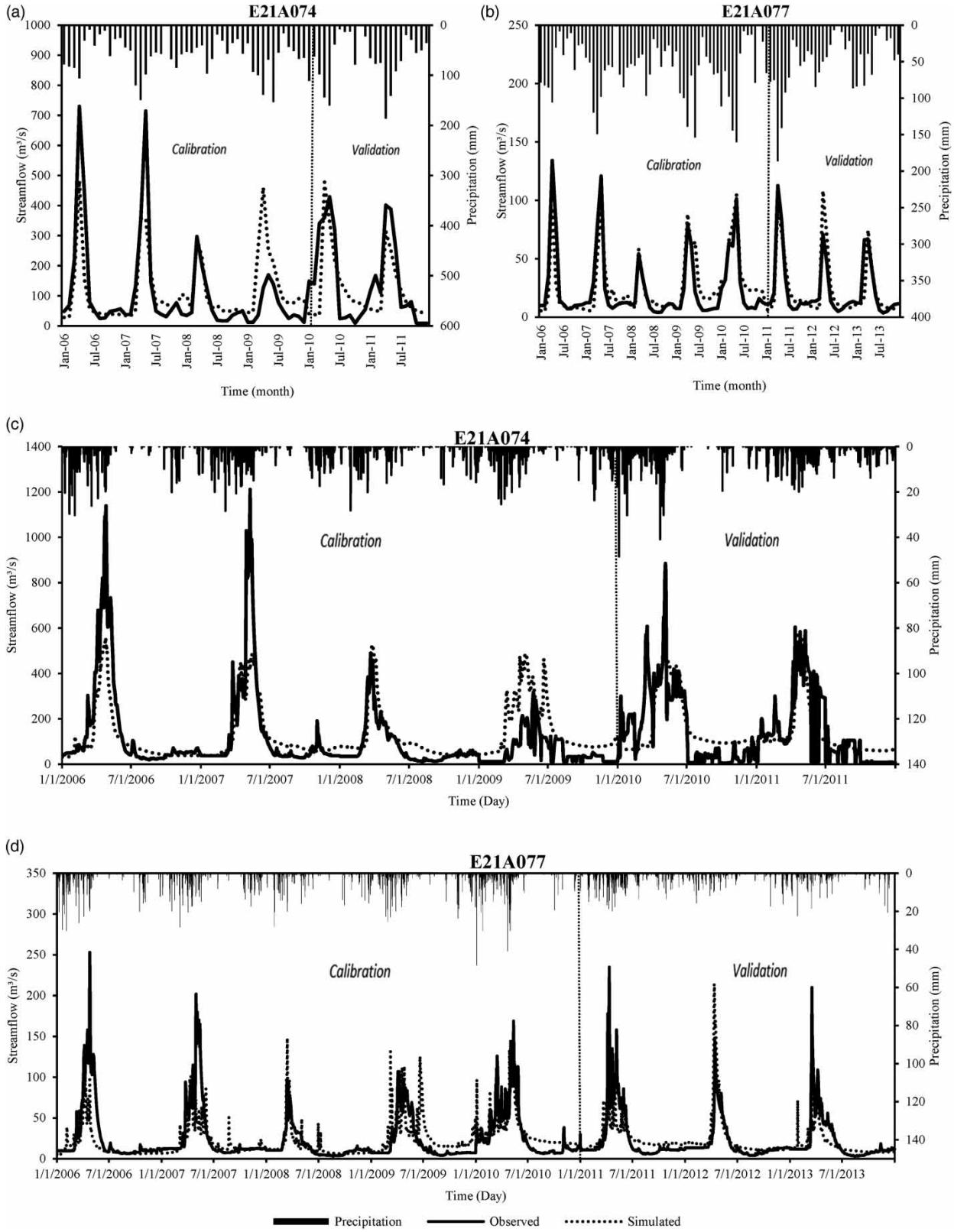

Figure 3 | Monthly observed streamflow versus simulated streamflow at the stations E21A074 (a) and E21A077 (b). Daily observed streamflow versus simulated streamflow at the stations E21A074 (c) and E21A077 (d).

Table 6 | Performance of the SWAT model for daily and monthly streamflow prediction for the stations E21A077 and E21A074

			Streamflow				
			NSE	R^2	PBIAS %	p-factor	r-factor
Monthly	E21A074	Calibration (2006–2009)	0.57	0.57	−7.4	0.65	1.08
		Validation (2010–2011)	0.50	0.53	15.6	0.54	1.31
	E21A077	Calibration (2006–2010)	0.77	0.77	−6.6	0.72	1.14
		Validation (2011–2013)	0.75	0.78	−3.1	0.86	1.22
Daily	E21A074	Calibration (2006–2009)	0.56	0.57	−15.0	0.80	1.11
		Validation (2010–2011)	0.55	0.56	1.20	0.42	0.79
	E21A077	Calibration (2006–2010)	0.45	0.46	7.7	0.74	0.90
		Validation (2011–2013)	0.50	0.50	1.20	0.62	0.57

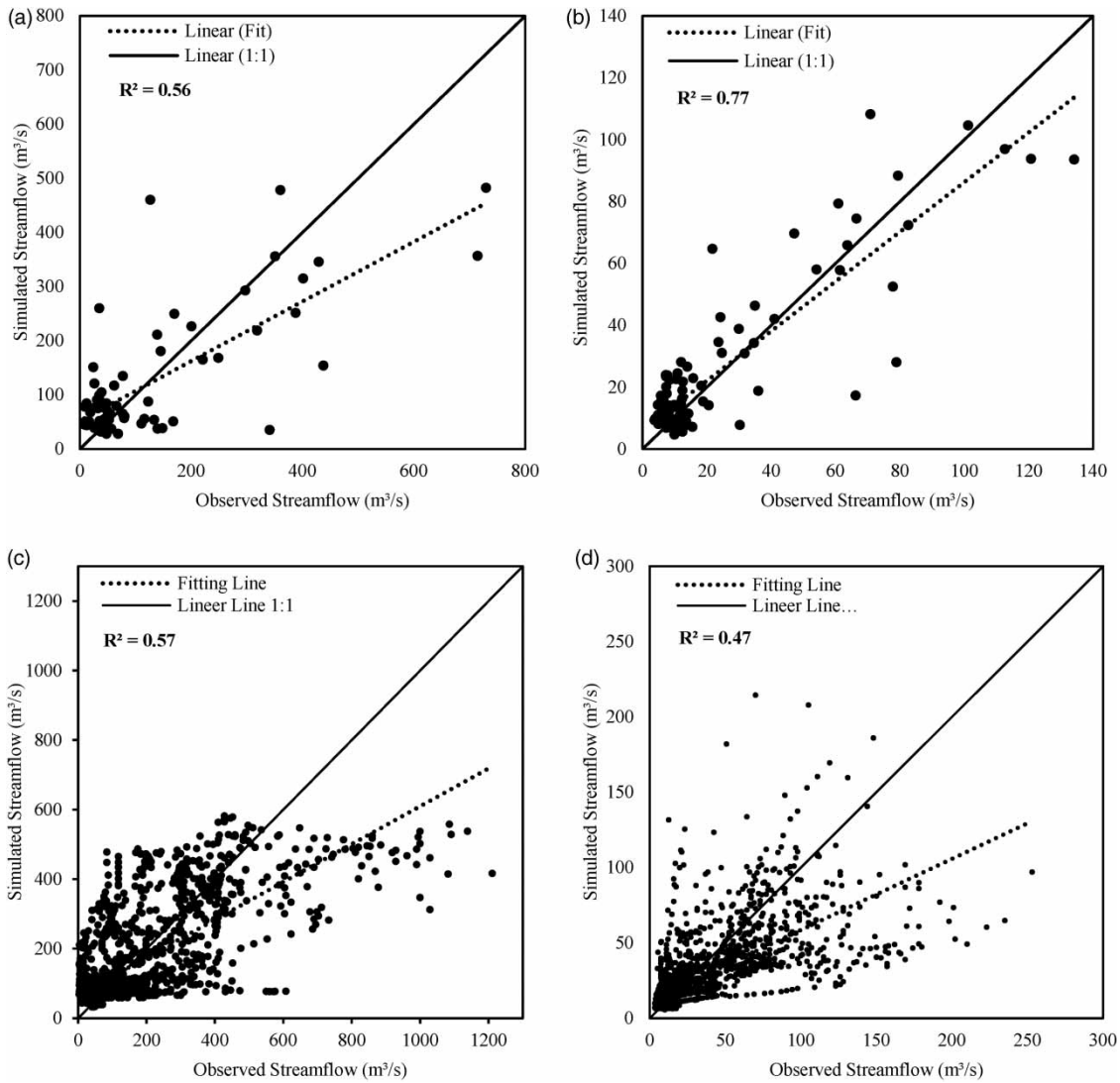

Figure 4 | Scatterplots of monthly (a) E21A074 and (b) E21A077 and daily (c) E21A074 and (d) E21A077 observed streamflow versus simulated streamflow during calibration and validation.

Table 7 | Performance of the SWAT model for monthly sediment yield prediction for the stations E21A074 and E21A077

		Sediment				
		NSE	R^2	PBIAS (%)	p-factor	r-factor
E21A074	Calibration (2006–2009)	0.54	0.67	−33.8	0.83	2.38
	Validation (2010–2011)	0.69	0.68	4.6	0.42	0.43
E21A077	Calibration (2006–2010)	0.62	0.68	−3.2	0.77	0.79
	Validation (2011–2013)	0.35	0.56	−77.2	0.20	0.49

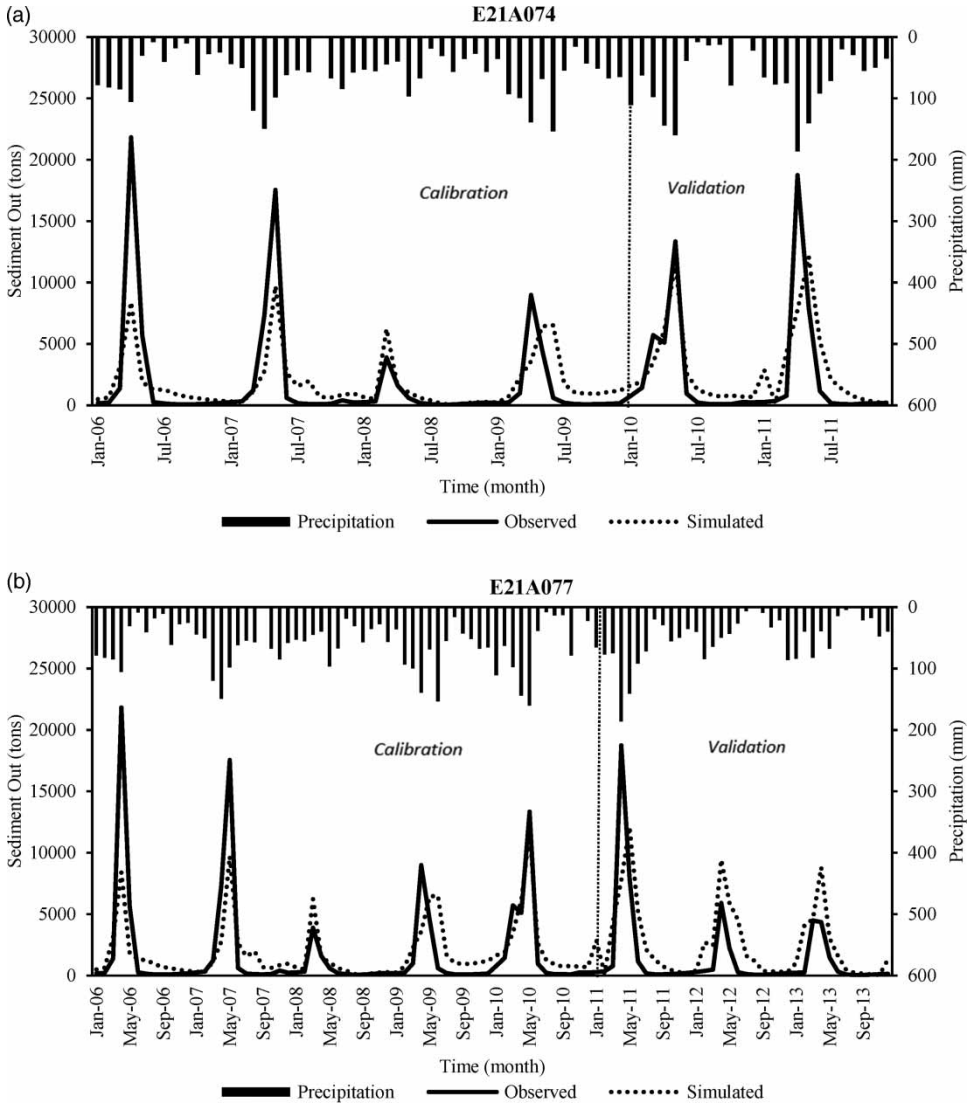

Figure 5 | Observed and simulated monthly sediment load at (a) E21A074 and (b) E21A077.

(10–20 t/ha/y), and very severe (>20 t/ha/y), based on the General Directorate Combating Desertification and Erosion (CEM 2018). The relationship between rainfall, runoff, and sediment yield have been described in Figure 7 showing that the rainfall, runoff, and sediment yield had the highest value during the wet period of the watershed from March to May. The maximum rainfall (118.36 mm) observed in April whereas the peak values of runoff and sediment yield observed in May. It is noted from these findings, that runoff could be a more efficient factor the produce sediment yield than rainfall. Similarly, a study by Dutta

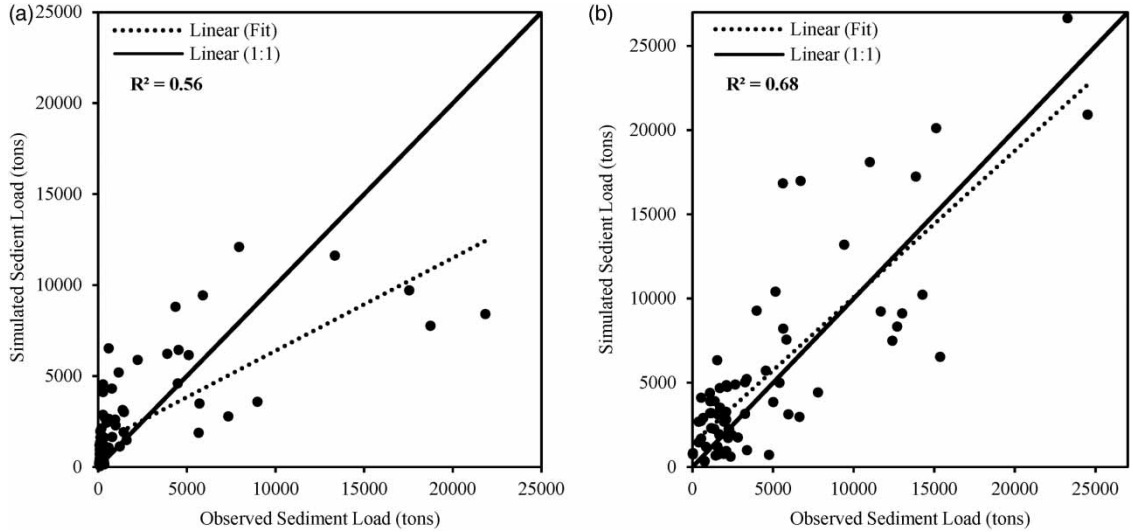

Figure 6 | Scatterplot of monthly observed versus simulated sediment load for the stations (a) E21A074 and (b) E21A077.

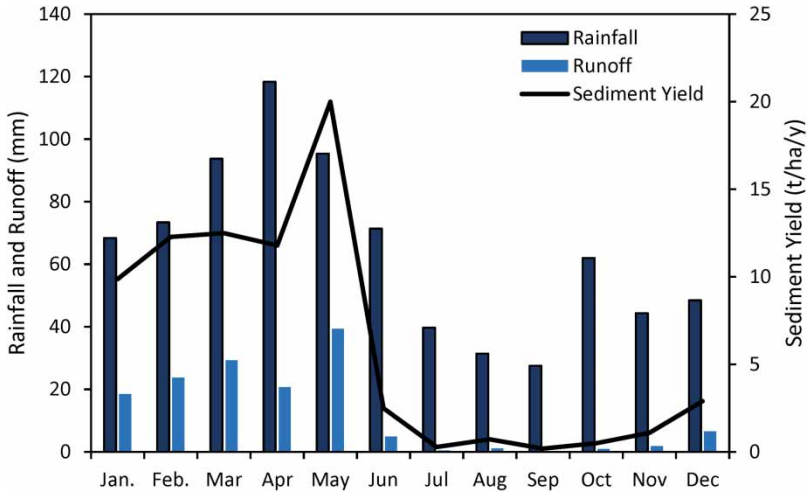

Figure 7 | The monthly patterns of rainfall, runoff and sediment yield.

& Sen (2018) also indicated that most of the sediment yield occurred by surface runoff during the intense rainfall session, whereas the peak of the sediment yield occurred after the rainfall cessation. It can be assumed that rainfall and runoff could be driven factors for sediment yield as seen in their trend from Figure 7. To address water management challenges, it is important to examine and quantify the components (precipitation, surface runoff, actual and potential evapotranspiration, and lateral flow) of hydrological processes that occur within the area of interest (Nasiri *et al.* 2020) and the SWAT model capable to estimates these hydrological components. The average annual water balance components were found as precipitation 774.5 mm, surface runoff 129 mm, actual evapotranspiration 494.1 mm, potential evapotranspiration 1,077.4 mm, lateral flow 7.06 mm, and total water yield 189.45 mm. Actual evapotranspiration (ET) generated the most water loss from the watershed, accounting for around 64% of total water loss. Lateral flow generated lowest share of water balance components as 0.9%.

The average annual sediment loads obtained from the model was 13,471 tons at the station E21A074 while 3,140 tons at E21A077. For the sub-basin-based analysis, the average sediment yield was found as 6.44 t/ha/y. The highest average sediment yield was observed at sub-basin #74 and sub-basin #76 with the values of 32.57 and 24.62 t/ha/y, respectively. The

lowest average sediment yield was found at the sub-basin #118 with the value of 0.78 t/ha/y. These results suggest that the maximum sediment yield occur on the watershed with a steep slope similar to results reported for Dokan Dam Reservoir in Northern Iraq (Ezz-Aldeen *et al.* 2018) and non-agricultural land such as barren and pasture. Spatial analysis indicated that a total of 3.9% of the basin is under very severe soil erosion categories while 21.3% of severe, 31.3% is moderate, 43% is slight, and 0.5% is very slight soil erosion condition (Figure 8(a)). Since there are many sub-watersheds based factors affecting soil losses such as land use/cover, soil type, and slope, Figure 9 was created to see these effects on soil erosion.

Runoff is one of the main factors that produce sediment yield. The maximum runoff was observed at the sub-watershed 139 with 46.11 mm, and the next sub-watershed 137 with 46.08 mm. The maximum average sediment yield was also obtained at the sub-watershed 76 with 42.5 mm runoff value. It is seen from Figure 8 that generally, the sediment yield value is high in the sub-watersheds where the runoff is high. The correlation coefficient between monthly average surface runoff and sediment yield was high ($R^2 = 0.98$) and statistically significant ($P < 0.05$). Similar results also indicated by Mosbahi & Benabdallah (2013) and Tibebe & Bewket (2011), that estimated sediment yield were generally higher where the runoff generation was the higher in the watershed. Figure 9(a) indicates that 61% of barren land was under very severe (48%) and severe (13%) soil erosion class, whereas 31% of forest area, 27% of pasture area, and 10% of agricultural area are under very severe soil erosion conditions. A total of 73% of agricultural area on the watershed was under the very slight (47%) and slight (26%) soil erosion class. The average soil erosion on the total area of barren land is 13.7 t/ha/y, while 5.8 t/ha/y in the agricultural area. These results show that the lowest soil erosion occurred in the agricultural area while the highest was seen in the barren area. The reason for that the cover factor has an influence on the soil erosion. Hence, in barren areas, there is no vegetation cover meanwhile in agricultural areas the vegetation provides a protection of soil.

The results were analyzed at the sub-watershed scale and found that especially the sub-watersheds 65, 66, 74, 75, 76, 137, and 139 produced more values for runoff, sediment yield, and soil erosion. These findings will guide decision-makers on the watershed management by focusing on these areas to take a precaution. With these measures to be taken, the sustainability of the basin will be ensured and less sediment transport will contribute to the economic life of the dams.

Figure 9(b) shows the ratio of soil erosion for the different soil types on the watershed. Loam soil texture covers 84% of the total watershed area and 18% of this area is in the category of very severe soil erosion. The rest of the watershed (16%) is a clay-loam texture with very severe (35%), severe (34%) soil erosion classes. The average sediment yield is higher in the Clay-Loam soil group (10.24 t/ha/y) than the Loam soil group (5.89 t/ha/y) since mostly Clay-Loam soils is located the downstream area where the mostly sediment yield occurred. Since the other factors such as rainfall erositivity, soil cover, land slope, and management practices have a major influence on soil erosion, it can not concluded that soil type is the most important driver in soil erosion. Similar results reported by Ricci *et al.* (2018). It is expected in Figure 9(c) that a higher value of slope produces more soil loss. 21% of the total area of the basin has a slope of greater than 25%, while 62% of its under the very severe (30%) and severe (32%) soil erosion class. In addition, the average sediment yield on a slope greater than 25% was

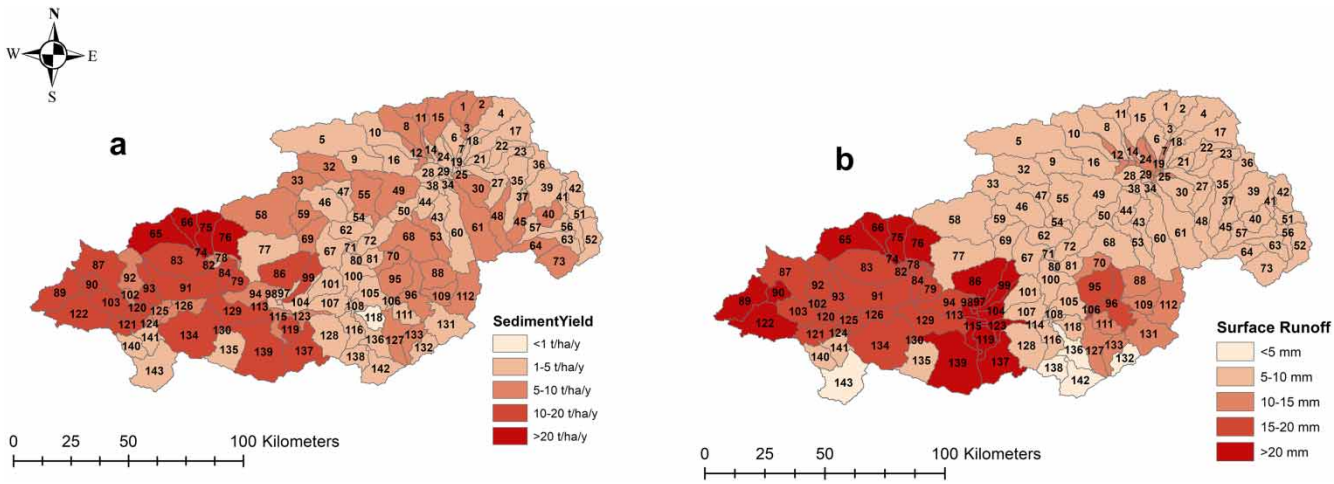

Figure 8 | An illustration of sub-watershed scales of (a) sediment yield and (b) surface runoff at the study area.

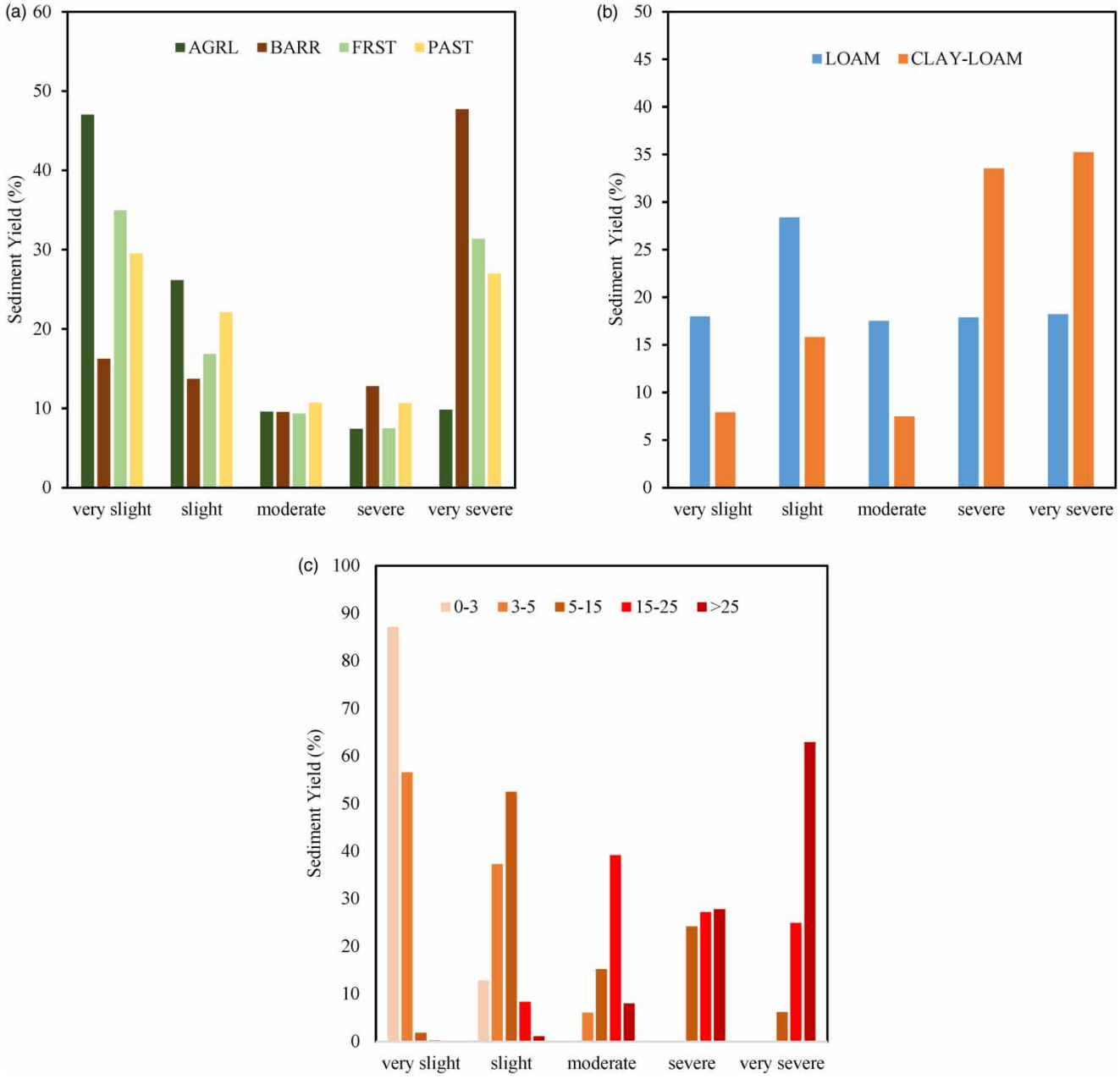

Figure 9 | The percentage of the sediment yield (%) by (a) land use, (b) soil type, and (c) terrain slope.

found as 18.5 t/ha, and on the slope of 15–25% as 9.54 t/ha, and with the lowest value as 0.38 t/ha on the slope of 0–3%. It can be concluded that slopes have an influence on sediment yield similar to results reported the study by Yuan & Forshay (2019). With all these findings from the figures and the results of sediment yields, it can be assumed that soil erosion is quite dependent on land use and soil type.

4. CONCLUSION

This study tried to demonstrate the performance of the SWAT model for estimating streamflow, sediment yield, and identification of soil erosion-prone areas in the Murat River basin, which is a part of the Euphrates-Tigris basin, the largest basin in Turkey. First, the sensitivity parameters were selected by using the Latin Hypercube One-Factor-At-A-Time (LH-OAT) algorithm and found the CN2 as the most sensitive parameter for daily and monthly streamflow. Then, the

model was calibrated and validated for both streamflow and sediment yield by using the SWAT-CUP program and compared with the data obtained from two gaging stations. Based on the statistical results, NSE, R^2, and PBIAS, the SWAT model was revealed to be a reliable tool to estimate streamflow and sediment yield in the Murat River Basin.

Terrain slope was found having a great influence on soil erosion. 63% of the area with a slope of greater than 25% are in the very severe erosion class. The hydrological components were analyzed based on the annual average values obtained from the SWAT model. Actual evapotranspiration (ET) generated most water loss from the watershed, accounting for around 64% of total water loss. The spatial distribution of soil erosion at the sub-watershed scale was also analyzed and the generated soil erosion map can clearly illustrate the prioritization of the basin's erosion-prone areas. The barren land is mostly observed in the area with a slope greater than 25% and consequently, sediment yield and soil erosion values are excessive. The average sediment yield was obtained as 13.72 t/ha/y on barren land use. Especially, the sub-watersheds 65, 66, 74, 75, 76, 137, and 139 produce a high amount of surface runoff, and sediment yield, so precautions should be focused on these areas. Indeed, sediment yield mostly observed in the downstream part of the basin. The findings of this study can help watershed managers to plan about where the best management techniques and conservation measures can be applied efficiency. Because of limited spatial studies about soil erosion and sediment yield in the Murat River Basin, this study will guide researchers who will work in this basin and nearby. Besides, the model could be also applied in future research to determine the impact of climate change on water resources, soil erosion, and land use.

ACKNOWLEDGEMENT

This paper has been derived from the doctoral dissertation of Erkan Karakoyun.

AUTHOR CONTRIBUTIONS

Conceptualization, Methodology, Software, Writing first draft: E.K. Visualization, Review and Editing, Supervision: N.K.

DATA AVAILABILITY STATEMENT

All relevant data are included in the paper or its Supplementary Information.

CONFLICT OF INTEREST

The authors declare there is no conflict.

REFERENCES

Abbaspour, K. C. 2015 *SWAT-CUP: SWAT Calibration and Uncertainty Programs – A User Manual*. Eawag: Swiss Federal Institute of Aquatic Science and Technology. https://doi.org/10.1007/s00402-009-1032-4.

Abbaspour, K. C. 2022 The fallacy in the use of the 'best-fit' solution in hydrologic modeling. *Science of the Total Environment* **802**, 149713. https://doi.org/10.1016/j.scitotenv.2021.149713.

Abbaspour, K. C., Johnson, C. A. & van Genuchten, M. T. 2004 Estimating uncertain flow and transport parameters using a sequential uncertainty fitting procedure. *Vadose Zone Journal* **3** (4), 1340–1352. https://doi.org/10.2113/3.4.1340.

Abbaspour, K. C., Yang, J., Maximov, I., Siber, R., Bogner, K., Mieleitner, J., Zobrist, J. & Srinivasan, R. 2007 Modelling hydrology and water quality in the pre-alpine/alpine Thur watershed using SWAT. *Journal of Hydrology* **333** (2–4), 413–430. https://doi.org/10.1016/j.jhydrol.2006.09.014.

Abbaspour, K. C., Rouholahnejad, E., Vaghefi, S., Srinivasan, R., Yang, H. & Kløve, B. 2015 A continental-scale hydrology and water quality model for Europe: calibration and uncertainty of a high-resolution large-scale SWAT model. *Journal of Hydrology* **524**, 733–752. https://doi.org/10.1016/j.jhydrol.2015.03.027.

Abbaspour, K. C., Vaghefi, S. A. & Srinivasan, R. 2017 A guideline for successful calibration and uncertainty analysis for soil and water assessment: a review of papers from the 2016 international SWAT conference. *Water (Switzerland)* **10** (1). https://doi.org/10.3390/w10010006.

Abdelwahab, O. M. M., Ricci, G. F., De Girolamo, A. M. & Gentile, F. 2018 Modelling soil erosion in a Mediterranean watershed: comparison between SWAT and AnnAGNPS models. *Environmental Research* **166**, 363–376. https://doi.org/10.1016/j.envres.2018.06.029.

Abouabdillah, A., White, M., Arnold, J. G., De Girolamo, A. M., Oueslati, O., Maataoui, A. & Lo Porto, A. 2014 Evaluation of soil and water conservation measures in a semi-arid river basin in Tunisia using SWAT. *Soil Use and Management*, 1–11. https://doi.org/10.1111/sum.12146.

Akiner, M. E. & Akkoyunlu, A. 2012 Modeling and forecasting river flow rate from the Melen Watershed, Turkey. *Journal of Hydrology* **456–457**, 121–129. https://doi.org/10.1016/j.jhydrol.2012.06.031.

Alemayehu, D., Srinivasan, R. & Daggupati, P. 2014 Application of soil and water assessment tool model to estimate sediment yield in Kaw Lake. *American Journal of Environmental Sciences* **10** (6), 530–545. https://doi.org/10.3844/ajessp.2014.530.545.

Arnold, J. G., Srinivisan, R., Muttiah, R. S. & Williams, J. R. 1998 Large area hydrological modeling and assessment part I: model development. *Journal of American Water Resources Association* **34** (1), 73–89. https://doi.org/10.1016/S0899-9007(00)00483-4.

Arnold, J. G., Kiniry, J. R., Srinivasan, R., Williams, J. R., Haney, E. B. & Neitsch, S. L. 2012 *Soil & Water Assessment Tool. Input/Output Documentation Version 2012*. Texas Water Resources Institute.

Ayele, G. T., Teshale, E. Z., Yu, B., Rutherfurd, I. D. & Jeong, J. 2017 Streamflow and sediment yield prediction for watershed prioritization in the upper Blue Nile river basin, Ethiopia. *Water (Switzerland)* **9** (10). https://doi.org/10.3390/w9100782.

Beskow, S., Mello, C. R., Norton, L. D., Curi, N., Viola, M. R. & Avanzi, J. C. 2009 Soil erosion prediction in the Grande River Basin, Brazil using distributed modeling. *Catena* **79** (1), 49–59. https://doi.org/10.1016/J.CATENA.2009.05.010.

Borrelli, P., Alewell, C., Alvarez, P., Alexandre, J., Anache, A., Baartman, J., Ballabio, C., Bezak, N., Biddoccu, M., Cerdà, A., Chalise, D., Chen, S., Chen, W., Maria, A., Girolamo, D., Desta, G., Deumlich, D., Diodato, N., Efthimiou, N., Erpul, G., Fiener, P., Freppaz, M., Gentile, F., Gericke, A., Haregeweyn, N., Hu, B., Jeanneau, A., Kaffas, K., Kiani-harchegani, M., Lizaga, I., Li, C., Lombardo, L., López-vicente, M., Lucas-borja, M. E., Märker, M., Matthews, F., Miao, C., Modugno, S., Möller, M., Naipal, V., Nearing, M., Owusu, S., Panday, D., Patault, E., Valeriu, C., Poggio, L., Portes, R., Quijano, L., Reza, M., Renima, M., Francesco, G., Rodrigo-comino, J., Saia, S., Nazari, A., Schillaci, C., Syrris, V., Soo, H., Noses, D., Tarso, P., Teng, H., Thapa, R., Vantas, K., Vieira, D., Yang, J. E., Yin, S., Antonio, D., Zhao, G. & Panagos, P. 2021 Soil erosion modelling: a global review and statistical analysis. *Science of the Total Environment Journal* **780**. https://doi.org/10.1016/j.scitotenv.2021.146494.

Briak, H., Moussadek, R., Aboumaria, K. & Mrabet, R. 2016 Assessing sediment yield in Kalaya gauged watershed (Northern Morocco) using GIS and SWAT model. *International Soil and Water Conservation Research* **4** (3), 177–185. https://doi.org/10.1016/j.iswcr.2016.08.002.

CEM 2018 *DEMİS Türkiye Su Erozyonu İstatistikleri, Teknik Özet*. Çölleşme ve Erozyonla Mücadele Genel Müdürlüğü Yayınları, Ankara, Türkiye.

Chakrabortty, R. & Chandra, S. 2020 Assessing the importance of static and dynamic causative factors on erosion potentiality using SWAT, EBF with uncertainty and plausibility, logistic regression and novel ensemble model in a sub-tropical environment. *Journal of the Indian Society of Remote Sensing* **48** (5), 765–789. https://doi.org/10.1007/s12524-020-01110-x.

Chakrabortty, R., Pradhan, B., Mondal, P. & Pal, S. C. 2020 The use of RUSLE and GCMs to predict potential soil erosion associated with climate change in a monsoon-dominated region of eastern India. *Arabian Journal of Geosciences* **13** (1073), 1–20. https://doi.org/10.1007/s12517-020-06033-y.

Chakrabortty, R., Chandra, S. & Alireza, P. 2022 Water-induced erosion potentiality and vulnerability assessment in Kangsabati river basin, eastern India. *Environment, Development and Sustainability* **24** (3), 3518–3557. https://doi.org/10.1007/s10668-021-01576-w.

Chandra, S. & Rabin, P. 2019 Modeling of water induced surface soil erosion and the potential risk zone prediction in a sub-tropical watershed of Eastern India. *Modeling Earth Systems and Environment* **5** (2), 369–393. https://doi.org/10.1007/s40808-018-0540-z.

CORINE 2012 *Copernicus Land Monitoring Service; CORINE Land Cover: Copenhagen, Denmark, 2012*. Available from: https://land.copernicus.eu/pan-european/corine-land-cover (accessed on 25 October 2020).

Cuceloglu, G., Abbaspour, K. C. & Ozturk, I. 2017 Assessing the water-resources potential of Istanbul by using a soil and water assessment tool (SWAT) hydrological model. *Water (Switzerland)* **9** (10). https://doi.org/10.3390/w9100814.

Daramola, J., Ekhwan, T. M., Mokhtar, J., Lam, K. C. & Adeogun, G. A. 2019 Estimating sediment yield at Kaduna watershed, Nigeria using soil and water assessment tool (SWAT) model. *Heliyon* **5** (7), e02106. https://doi.org/10.1016/j.heliyon.2019.e02106.

De Girolamo, A. M., Barca, E., Leone, M. & Lo Porto, A. 2022 Impact of long-term climate change on flow regime in a Mediterranean basin. *Journal of Hydrology: Regional Studies* **41**, 101061. https://doi.org/10.1016/j.ejrh.2022.101061.

Duru, U., Arabi, M. & Wohl, E. E. 2018 Modeling stream flow and sediment yield using the SWAT model: a case study of Ankara River basin, Turkey. *Physical Geography* **39** (3), 264–289. https://doi.org/10.1080/02723646.2017.1342199.

Dutta, S. & Sen, D. 2018 Application of SWAT model for predicting soil erosion and sediment yield. *Sustainable Water Resources Management* **4** (3), 447–468. https://doi.org/10.1007/s40899-017-0127-2.

Esri 2019 *ArcGIS Desktop: Release (10.7)*. Environmental Systems Research Institute, Redlands, CA.

Ezz-Aldeen, M., Hassan, R., Ali, A., Al-Ansari, N. & Knutsson, S. 2018 Watershed sediment and its effect on storage capacity: case study of Dokan Dam Reservoir. *Water (Switzerland)* **10** (7), 1–16. https://doi.org/10.3390/w10070858.

FAO/UNESCO Food and Agriculture Organization – United Nations Educational, Scientific and Cultural Organization, FAO Digital Soil Map of the World (DSMW). Available from: http://www.fao.org/geonetwork/srv/ (accessed 25 October 2020).

Gull, S., Manzoor, A. & Dar, A. M. 2017 Prediction of stream flow and sediment yield of Lolab watershed using SWAT model. *Hydrology: Current Research* **08** (01). https://doi.org/10.4172/2157-7587.1000265.

Gupta, H. V., Sorooshian, S. & Yapo, P. O. 1999 Status of automatic calibration for hydrologic models: comparison with multilevel expert calibration. *Journal of Hydrologic Engineering* **4** (2), 135–143. https://doi.org/10.1061/(ASCE)1084-0699(1999)4:2(135).

Guzel, C. 2010 *Application of SWAT Model in a Watershed in Turkey*. *MSc Thesis*, Istanbul Technical University.

Imamoglu, A. & Dengiz, O. 2017 Determination of soil erosion risk using RUSLE model and soil organic carbon loss in Alaca catchment (Central Black Sea region, Turkey). *Rendiconti Lincei. Scienze Fisiche e Naturali* **28**, 11–23. https://doi.org/10.1007/s12210-016-0556-0.

Jakada, H. & Chen, Z. 2020 An approach to runoff modelling in small karst watersheds using the SWAT model. *Arabian Journal of Geosciences* **13** (8). https://doi.org/10.1007/s12517-020-05291-0.

Jodar-Abellan, A., Valdes-Abellan, J., Pla, C. & Gomariz-Castillo, F. 2019 Impact of land use changes on flash flood prediction using a sub-daily SWAT model in five Mediterranean ungauged watersheds (SE Spain). *Science of the Total Environment* **657**, 1578–1591. https://doi.org/10.1016/j.scitotenv.2018.12.034.

Juracek, K. E. & Stiles, T. C. 2010 The role of reservoir sediment studies in the TMDL process in Kansas. *Proceedings of the Water Environment Federation* **2003** (4), 1091–1102. https://doi.org/10.2175/193864703784828273.

Koycegiz, C., Buyukyildiz, M. & Kumcu, S. Y. 2021 Spatio-temporal analysis of sediment yield with a physically based model for a data-scarce headwater in Konya Closed Basin, Turkey. *Water Science and Technology: Water Supply* **21** (4), 1752–1763. https://doi.org/10.2166/WS.2021.016.

Mahmood, K. 1987 *Reservoir Sedimentation: Impact, Extent, Mitigation. World Bank Technical Report No: 71*.

Moriasi, D. N., Arnold, J. G., Van Liew, M. W., Bingner, R. L., Harmel, R. D. & Veith, T. 2007 Model evaluation guidelines for systematic quantification of accuracy in watershed simulations. *Transactions of the ASABE* **50** (3), 885–900. https://doi.org/10.1234/590.

Morris, G. L. & Fan, J. 1998 *Reservoir Sedimentation Handbook*. McGraw-Hill Book Co., New York.

Mosbahi, M. & Benabdallah, S. 2013 Assessment of soil erosion risk using SWAT model. *Arabian Journal of Geosciences* **6**, 4011–4019. https://doi.org/10.1007/s12517-012-0658-7.

Mutchler, C. K., Murphree, C. E. & McGregor, K. C. 1998 Laboratory and field plots for soil erosion studies. *Soil Erosion Research Methods*. Soil and Water Conservation Society, New York, pp. 9–36.

NASA 2019 *NASA/METI/AIST/Japan Space Systems and U.S./Japan ASTER Science Team. 2019 ASTER Global Digital Elevation Model V003 [Data set]. NASA EOSDIS Land Processes DAAC*. Available from: https://lpdaac.usgs.gov/products/astgtmv003/ (accessed 25 October 2020).

Nash, J. E. & Sutcliffe, J. V. 1970 River flow forecasting through conceptual models part I – a discussion of principles. *Journal of Hydrology* **10** (3), 282–290. https://doi.org/10.1016/0022-1694(70)90255-6.

Nasiri, S., Ansari, H. & Ziaei, A. N. 2020 Simulation of water balance equation components using SWAT model in Samalqan Watershed (Iran). *Arabian Journal of Geosciences* **13** (11). https://doi.org/10.1007/s12517-020-05366-y.

Neitsch, S. L., Arnold, J. G., Kiniry, J. R. & Williams, J. R. 2005 *Soil and Water Assessment Tool Theoretical Documentation Version 2005*.

Pal, S. C. & Chakrabortty, R. 2019 Simulating the impact of climate change on soil erosion in sub-tropical monsoon dominated watershed based on RUSLE, SCS runoff and MIROC5 climatic model. *Advances in Space Research*. https://doi.org/10.1016/j.asr.2019.04.033.

Pal, C. S. & Shit, M. 2017 Application of RUSLE model for soil loss estimation of Jaipanda watershed, West Bengal. *Spatial Information Research* **25** (3), 399–409. https://doi.org/10.1007/s41324-017-0107-5.

Pal, C. S., Chakrabortty, R., Roy, P., Chowdhuri, I., Das, B., Saha, A. & Shit, M. 2021 Changing climate and land use of 21st century influences soil erosion in India. *Gondwana Research* **94**, 164–185. https://doi.org/10.1016/j.gr.2021.02.021.

Panagos, P., Borrelli, P., Poesen, J., Ballabio, C., Lugato, E., Meusburger, K., Montanarella, L. & Alewell, C. 2015 The new assessment of soil loss by water erosion in Europe. *Environmental Science and Policy* **54**, 438–447. https://doi.org/10.1016/j.envsci.2015.08.012.

Panagos, P., Ballabio, C., Himics, M., Scarpa, S., Matthews, F., Bogonos, M., Poesen, J. & Borrelli, P. 2021 Projections of soil loss by water erosion in Europe by 2050. *Environmental Science and Policy* **124**, 380–392. https://doi.org/10.1016/j.envsci.2021.07.012.

Panda, C., Das, D. M., Raul, S. K. & Sahoo, B. C. 2021 Sediment yield prediction and prioritization of sub-watersheds in the Upper Subarnarekha basin (India) using SWAT. *Arabian Journal of Geosciences* **14** (9). https://doi.org/10.1007/s12517-021-07170-8.

Peker, I. B. & Sorman, A. A. 2021 Application of SWAT using snow data and detecting climate change impacts in the mountainous eastern regions of Turkey. *Water (Switzerland)* **13** (14). https://doi.org/10.3390/w13141982.

Qi, J., Zhang, X., Yang, Q., Srinivasan, R., Arnold, J. G., Li, J., Waldholf, S. T. & Cole, J. 2020 SWAT ungauged: water quality modeling in the Upper Mississippi River Basin. *Journal of Hydrology* **584**. https://doi.org/10.1016/j.jhydrol.2020.124601.

Ricci, G. F., De Girolamo, A. M., Abdelwahab, O. & Gentile, F. 2018 Identifying sediment source areas in a Mediterranean watershed using the SWAT model. *Land Degradation and Development* **29** (4), 1233–1248. https://doi.org/10.1002/ldr.2889.

Rodríguez-Blanco, M. L., Arias, R., Taboada-Castro, M. M., Nunes, J. P., Keizer, J. J. & Taboada-Castro, M. T. 2016 Sediment yield at catchment scale using the SWAT (Soil and Water Assessment Tool) model. *Soil Science* **181** (7). https://doi.org/10.1097/SS.0000000000000158.

Roy, P., Chakrabortty, R., Chowdhuri, I., Malik, S., Das, B. & Pal, S. C. 2020 *Development of Different Machine Learning Ensemble Classifier for Gully Erosion Susceptibility in Gandheswari Watershed of West Bengal, India*. Springer, Singapore. https://doi.org/10.1007/978-981-15-3689-2.

Runkel, R. L., Crawford, C. G. & Cohn, T. A. 2004 *Load Estimator (LOADEST): A FORTRAN Program for Estimating Constituent Loads in Streams and Rivers*. U.S. Geological Survey, Reston, Virginia 2328-7055.

Sohoulande Djebou, D. C. 2018 Assessment of sediment inflow to a reservoir using the SWAT model under undammed conditions: a case study for the Somerville reservoir, Texas, USA. *International Soil and Water Conservation Research* **6** (3), 222–229. https://doi.org/10.1016/j.iswcr.2018.03.003.

Tesema, T. A. & Leta, O. T. 2020 Sediment yield estimation and effect of management options on sediment yield of Kesem Dam Watershed, Awash Basin, Ethiopia. *Scientific African* **9**, e00425. https://doi.org/10.1016/j.sciaf.2020.e00425.

Tibebe, D. & Bewket, W. 2011 Surface runoff and soil erosion estimation using the Swat model in the Keleta Watershed, Ethiopia. *Land Degradation and Development* **22**, 551–564.

Tzoraki, O., De Girolamo, A. M., Gamvroudis, C. & Skoulikidis, N. 2015 Assessing the flow alteration of temporary streams under current conditions and changing climate by Soil and Water Assessment Tool model. *International Journal of River Basin Management*, 1–10. https://doi.org/10.1080/15715124.2015.1049182.

van Griensven, A. & Meixner, T. 2006 Methods to quantify and identify the sources of uncertainty for river basin water quality models. *Water Science and Technology* **53** (1), 51–59. https://doi.org/10.2166/WST.2006.007.

Van Liew, M. W. & Mittelstet, A. R. 2018 Comparison of three regionalization techniques for predicting streamflow in ungaged watersheds in Nebraska, USA using SWAT model. *International Journal of Agricultural and Biological Engineering* **11** (3), 110–119. https://doi.org/10.25165/j.ijabe.20181103.3528.

Vigiak, O., Malagó, A., Bouraoui, F., Vanmaercke, M. & Poesen, J. 2015 Science of the total environment adapting SWAT hillslope erosion model to predict sediment concentrations and yields in large basins. *Science of the Total Environment* **538**, 855–875. https://doi.org/10.1016/j.scitotenv.2015.08.095.

Williams, J. R. 1975 *Sediment-Yield Prediction with Universal Equation Using Runoff Energy Factor*.

Wu, Y. & Chen, J. 2012 Modeling of soil erosion and sediment transport in the East River Basin in southern China. *Science of The Total Environment* **441**, 159–168. https://doi.org/10.1016/J.SCITOTENV.2012.09.057.

Wuepper, D., Borrelli, P. & Finger, R. 2020 Countries and the global rate of soil erosion. *Nature Sustainability* **3** (1), 51–55. https://doi.org/10.1038/s41893-019-0438-4.

Yang, X., Liu, Q., He, Y., Luo, X. & Zhang, X. 2016 Comparison of daily and sub-daily SWAT models for daily streamflow simulation in the Upper Huai River Basin of China. *Stochastic Environmental Research and Risk Assessment* **30** (3), 959–972. https://doi.org/10.1007/s00477-015-1099-0.

Yıldırımer, S. 2018 *Borçka Barajı Havzasında Su Rejimi, Su Kalitesi ve Sediment Veriminin SWAT Kullanarak Belirlenmesi ve Modellenmesi*. PhD Dissertation, Artvin Coruh University.

Yuan, L. & Forshay, K. J. 2019 Using SWAT to evaluate streamflow and lake sediment loading in the Xinjiang river basin with limited data. *Water* **12**, 39. doi:10.3390/w12010039

Zare, M., Panagopoulos, T. & Loures, L. 2017 Simulating the impacts of future land use change on soil erosion in the Kasilian watershed, Iran. *Land Use Policy* **67**, 558–572. https://doi.org/10.1016/J.LANDUSEPOL.2017.06.028.

Zhang, X., Xu, Y. P. & Fu, G. 2014 Uncertainties in SWAT extreme flow simulation under climate change. *Journal of Hydrology* **515**, 205–222. https://doi.org/10.1016/j.jhydrol.2014.04.064.

First received 21 April 2022; accepted in revised form 13 November 2022. Available online 22 November 2022